CHAPTER 5

Histopathological & Biochemical Assessment using Developed Nano-formulation in Breast Cancer Rat Model

5.1. Introduction

Breast cancer is the leading cause of mortality [220] in females and constitutes around one-fourth of all cancer globally [253]. It is characterized by malignant, invasive breast cells that infiltrate beyond the affected organ [254]. Chemotherapy, radiation, and surgery are conventional treatment choices for cancer. However, mostly these therapies display high toxicity and poor specificity and are known to be less stable [255]. Recent advancements have seen immunotherapy, small molecule-based treatments, and combinations of these approaches [256]. On the same line, methotrexate (MTX) has been popularly used in various cancers such as breast, lung, cervical, and skin [242]. Its broad-spectrum efficacy in multiple diseases, from arthritis to cancer, makes it a very attractive drug. Besides, it also shows anti-inflammatory and immunomodulatory activities [257]. Methotrexate is a competitive inhibitor of an enzyme (dihydrofolate reductase) and acts by blocking folate binding sites [17]. The chemical structure of methotrexate is shown in Figure S3(b). Due to this, tetrahydrofolate production is inhibited, leading to the suppression of pyrimidine and purine production. This blocks the production of DNA and RNA, which are responsible for cancer cell growth [258]. Furthermore, MTX has the properties to inhibit the cytokines such as Tumor Necrosis Factor-α (TNF-α) and Interleukins (IL-1β & IL-6) [259]. Despite several advantages, MTX harms healthy cells, leading to hepatotoxicity, fibrosis, and cirrhosis [260]. These problems arise due to the low water solubility of MTX (0.01 mg/ml) [261], leading to poor drug bioavailability at

the desired place. Further, due to the small drug size, MTX retention time within the tumor is significantly less (2-10 h), reducing its efficacy [24]. Therefore, in cases where patients require high doses (up to 3 g/m^2 of body surface), it has limited use due to its side effect on the liver and kidney function. Even though numerous strategies have been employed to diminish the undesirable effects of methotrexate and enhance its efficacy [239,262], these drawbacks could be resolved by incorporating nanotechnology methods into the drug delivery system [263]. As a revolutionary drug delivery mechanism, nanotechnology offers opportunities to address problems with existing drug delivery techniques, such as lack of tumor cell selectivity, systemic toxicity, and poor solubility. Nanoparticles provide an innovative platform for targeting, high surface area, and the ability to control drug release[264,265]. Moreover, nanoparticles can increase selective distribution, enhance permeation across the biological barrier, and accumulate at the tumor site of the drugs [266]. One of the best methods to improve treatment effectiveness is using chitosan nanocarrier for drug delivery [267–269].

Furthermore, the initial step is to analyze tissue histology to explore any anticancer agent's mechanism of action and effect. Biochemical assays were used for toxicity assessment of the drug in the liver and kidney function biomarkers. Serum glutamic oxyacetic transaminase (SGOT) and serum glutamic pyruvic transaminase (SGPT) are enzymes involved in liver function. A significant increase in serum may indicate hepatotoxicity. Whereas kidney enzymes such as Alkaline Phosphatase (ALP), Urea, and Creatinine significantly increase may show nephrotoxicity. Besides this, pro-inflammatory cytokines also play an essential role in mammary tumor generation. Therefore, an Inflamed tumor microenvironment may typically consist of infiltrating immune cells (macrophages, neutrophils, and T-lymphocytes) and secretes growth factors, chemokines, and cytokines to which the tumor responds. Their serum

concentrations are crucial in determining how well cancer treatments work. Some cytokines, such as TNF-α and Interleukin (IL-1β, IL-6), may stimulate cancer cells and assist their proliferation and invasion. The study investigates the therapeutic potential of MTX-loaded chitosan nanoparticles at a low dose in an N-methyl N-nitrosourea-induced tumor rat model. Sprague-Dawley and Wistar-Furth rats are prone to transformation caused by chemical carcinogens in their mammary glands. N-methyl N-nitrosourea (MNU) and 7,12-dimethylbenz(a)anthracene (DMBA) are the two most often employed active chemicals that induce breast cancer [270]. The MNU animal model for breast carcinogenesis is a preclinical in-vivo model for evaluating drug efficacy and its therapeutic potential [271]. Most suitable induced models must be easy and quick to cause tumors and should have low mortality rates so that desired studies should be completed.

Developed nanotherapeutics efficacy has been evaluated using MNU-induced mammary tumors in rats. Nanotherapeutics is administered intravenously (i.v) through the tumor-bearing rat's tail vein and further assessed the pro-inflammatory biomarker using an ELISA assay kit. Additionally evaluated cytotoxic effects on different organs, primarily hepatic and renal function.

5.2 Experimental section

5.2.1 Animal grouping and treatment protocol

Female Sprague Dawley (SD) rat weight 130 ± 10 gm was used for this study. Animals were maintained in an animal house at the Department of Pharmaceutical IIT-BHU. Before the experiment, the animal was acclimated for a week at a temperature of 23 ±

2°C and a humidity level of 55 - 60% in a natural light/dark environment. It was also given to pelleted food and water ad libitum [235].

The 20 mg of N-methyl N-nitrosourea (Quiver Biotech Pvt Ltd Hyderabad, India) was dissolved immediately in 0.5 mL physiologic saline solution (0.9 % NaCl) before its use [272]. One dose of MNU was administered intraperitoneally (i.p) into the sterile air pouch 24 hours after sterilizing. For MNU-induced mammary cancer, the intraperitoneal approach is the most dependable, quick, and repeatable [273]. Twenty-four rats (II–V groups) received i.p administration of MNU. After the promotional stage (~ 42 days after the MNU induction), Six rats per group, animals were allocated into five groups at random as follows:

1) **Group I:** normal control group - left untreated and received saline only
2) **Group II:** Diseased control group - rats only received MNU
3) **Group III:** Meth-Cs-NPs treatment group – rats received MNU (ip) and Meth-Cs-NPs (equivalent dose 5 mg/kg of MTX) i.v
4) **Group IV:** Cs-NPs treatment group - rats received MNU and Cs-NPs (i.v), and
5) **Group V:** Drug control group (MTX) – rats received MNU and 5 mg/kg MTX body weight (i.v).

Throughout the experiment, rats' weights were measured every week. On alternate days, the tumor site was palpated to check for mammary gland growth and detect any visible tumor nodules. A digital vernier caliper measured the tumor volume on an altered day [237]. Treatment was started after the 8^{th} week of the single dose of MNU. Anticancer effects were performed in tumor-bearing rats. After the 6^{th} week of post-treatment, via retro-orbital plexus, blood samples were collected from each group into an EDTA-coated tube, and centrifugation at 1,000 g for 10 minutes at four °C temperature was used to separate the plasma for biochemical analysis.

5.2.2 Assessment of cytokines as a biomarker (ELISA)

To measure cytokine levels using Enzyme-Linked Immunosorbent Assays (manufactured by KRISHGEN Biosystems). The concentration of cytokines such as Tumor Necrosis Factor-α (TNF-α) and Interleukins (IL) (1β & 6) was determined by following the manufacturer protocol. And assessed the impact of methotrexate-loaded chitosan nanoparticles, and up or down-regulation of these cytokine levels in tumor-bearing rats. The lyophilized recombinant Tumor Necrosis Factor-α and Interleukin (1β & 6) were suspended in 600 µL of sterile water. The solution was then let to rest for 15 minutes, then gently stirred to make a 1000 pg/ml stock solution. From the stock solution, successive dilutions were performed to make working standard concentrations of 500, 250, 125, 62.5, 31.3, and 15.63 pg/mL. Then 96 well-plates were filled with 100 µL of each working concentration and serum from each treatment group (normal control, diseased control, and nanoparticles treatment group). To help cytokines become immobile, the well plate was covered and incubated for two hours at 18 to 25 °C. The immobilization is happened by the existence of cytokines in the sample and standard that are integrated with antibodies on the surface of 96-well plates. To get rid of unbound protein and antibodies, the well plates were rinsed with wash buffer and blotted four times with the help of blotting paper. Then, 100 µL of BIO-CONJ (biotin-conjugated) detection antibody was added to each well and incubated for an hour at 18 to 25 °C. After an hour of incubation, the immobilized interleukins in the wells are bound by the biotin-conjugated antibody. The well plate was washed four times before adding 100 µL streptavidin HRP enzyme and incubated for thirty minutes at 18 to 25 °C. The streptavidin HRP cytokines BIO-CONJ complex is formed by the covalent

integration of streptavidin-HRP enzymes with Tumor Necrosis Factor-α, Interleukin (1β, and 6) conjugated BIO-CONJ complex. Then well-plate was rinsed again, and 100 µL

3,3',5,5'-Tetramethylbenzidine (TMB) substrate was added. This was done at 18 to 25 °C for 15 minutes in the dark. The incubation causes the TMB to bind to the streptavidin HRP-proinflammatory cytokines-BIO-CONJ complex, which produces a blue color. After adding a hundred microliters of stop solution, the serum of the test sample turns yellow, showing the presence of TNF-α, Interleukins (1β, and 6). To quantitatively estimate pro-inflammatory cytokines, the absorbance was taken at 450 nm with the help of a Synergy H1 microplate reader (Figure 5.2).

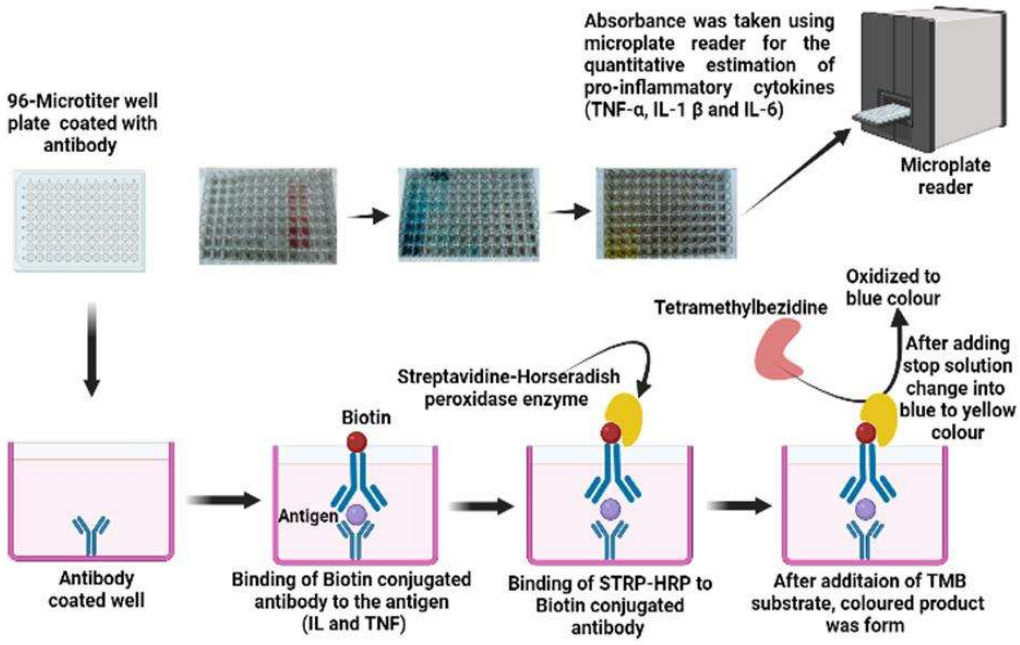

Figure 5.1: *Strategy of ELISA (Enzyme-linked immunosorbent assays) working protocol and assessment of cytokines; Tumor Necrosis Factor-α and Interleukins (IL-1β & IL-6)*

5.2.3 Assessment of renal and hepatic enzymatic function biomarkers

Liver function activity biomarkers, including Serum Glutamic Oxaloacetic Transaminase (SGOT) and Serum Glutamic Pyruvic Transaminase (SGPT), and kidney function activity biomarkers such as; Alkaline phosphate (ALP), Urea, and Creatinine levels were estimated in serum samples. Following the manufacturer's instructions, a commercially available standard kits (Erba) was utilized to determine the level of liver and kidney function biomarkers in the test sample using a biochemical analyzer (Erbachem 5 Plus).

5.2.4 Histopathological study

Rats were sacrificed, and their liver and kidneys were removed after the experiment. The tissues were immediately kept in a 10 % formalin solution for activation. Then the tissue is embedded into the paraffin and cut into a thin section of ~ 5 µm using a microtome. Then hematoxylin and eosin are used for staining the tissue for the histopathological analysis. A high-resolution microscope with 20X magnification was used to study any pathological changes in tissue.

5.2.5 Statistical analysis

One-way analysis of variance (ANOVA) with Dunnett's multiple comparison post-test was used to analyze differences between treatment groups relative to the control group. The findings of each experiment were given as mean, ± S.d, and duplicates of each experiment were run. Statistical significance was defined as a probability level of * $P < 0.05$, ** $P < 0.01$, and *** $P < 0.001$. Graph Pad Prism 5 was used to conduct the analysis.

5.3 Results and Discussion

5.3.1 Histopathology of mammary tumors (MNU-induced)

Benign or malignant tumors can be analyzed based on histology analysis. Histological studies were done on tumor sections using Haematoxylin and Eosin staining (H&E). According to a histopathological examination, all treated rats had mammary tumors and showed many histological patterns. The tumors were found in round, oval, and irregular shapes. The tumors that formed in the MNU-induced animals were fibroadenomas and adenocarcinomas with few adenomas. Carcinomas penetrated the surrounding tissues while retaining the gland's normal morphology. It was usually noted that there was a massive stromal reaction, as evidenced by inflammatory infiltration and fibrosis. Figure 5.2a demonstrates the histology of the normal rat mammary gland, showing the differentiation of the four layers into the epidermis (E), dermis (D), fat (F), and connective tissue (C). At the same time, Figure 5.2b represents the mammary parenchyma's early alterations after exposure to a carcinogen. The terminal end buds enlarge due to this intra-ductal proliferation or hyperplasia. It also results in a two-layer or more thickening of the epithelium lining. Furthermore, Figure 5.2c in-situ solid comedocarcinoma (DCIS) is characterized by centrally positioned necrotic debris and overstated ductal structures lined by a multilayered epithelium. The basement membrane is still intact. The involved ducts are distorted to variable grades depending on the expansion size. The stroma of each ductal structure was composed of dense fibrous tissue and displayed a distinct desmoplasia. Figure 5.2d, the tissue sections showed neoplastic cells that were actively growing in lobules grouped in solid sheets, frequently forming secondary lumina with various shapes, including round and irregular shapes that resembled sieves. Results show that most of the induced carcinoma was the cribriform type [272]. Large pleomorphic nuclei with distinct nucleoli and modest cytoplasm

characterize the malignant (atypical) cell. Histological analysis of tumor tissue from various groups reveals hyperchromatic with aberrant mitosis, tumor degeneration with necrotic tissues, and prominent infiltration of inflammatory cells.

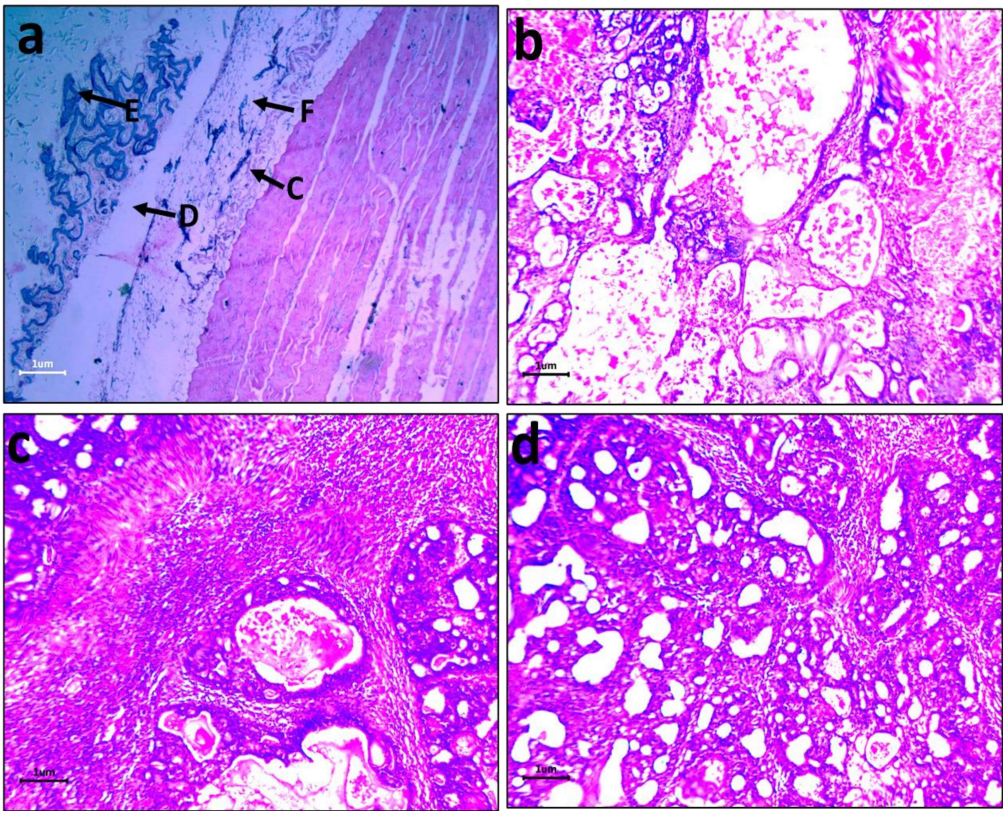

Figure 5.2: *Histopathology of mammary tumor of rat (MNU-induced) indicates the tumor generation with different tissue morphology;* ***(a)*** *Normal mammary gland tissue; Epidermis (E), Dermis (D), Fat (F), and Connective tissue (C),* ***(b)*** *Intra-ductal proliferation or hyperplasia,* ***(c)*** *Solid comedocarcinoma in situ (DCIS): Distended ductal formations lined by a multilayered epithelium and centrally situated necrotic material with the intact basement membrane, and* ***(d)*** *In situ solid cribriform carcinoma: The basement membrane is still entire, and there are solid sheets of cancerous cells with irregularly formed secondary lumina within the lobule. H&E staining, bar size 1µm with 10X magnification.*

5.3.2 Role of pro-inflammatory cytokines in tumor generation

This analysis assesses cytokine levels and the chemotherapeutic efficacy of MTX-loaded nanoparticles (Meth-Cs-NPs) against MNU-induced mammary tumors in rats. Chronic inflammation sets off cellular processes that may facilitate carcinogenesis and the malignant transformation of cells. It has been demonstrated that several inflammatory mediators have a role in the development and spread of cancer. According to reports, the pro-inflammatory cytokines such as; Tumor Necrosis Factor-α (TNF-α) and Interleukins (IL) (1β & 6) serve as significant inflammation markers during the pathophysiology of breast cancer [259]. Table 5.1; shows that TNF-α levels (36.9 ± 5 pg/mL) significantly ($P< 0.0001$) increased in the disease group. However, in the Meth-Cs-NP group, the TNF-α level (17.31 ± 1.15 pg/mL) showed an insignificant drop. Whereas a significant ($P < 0.001$) reduction in TNF-α level in free MTX (21 ± 1.87 pg/mL) and Cs-NPs (33.09 ± 1.25) treatment groups, respectively (Figure 5.3a). Based on the findings, it was found that breast carcinomas have high levels of the inflammatory cytokine TNF-α [274]. The diseased control group showed IL-1β levels (1540 ± 131.1 pg/mL) in serum increased significantly ($P < 0.0001$). After the administration of Meth-Cs-NPs (treatment group), the IL-1β level (433.3 ± 66.5 pg/mL) decreased significantly ($P < 0.01$). Whereas in the case of free MTX, the IL-1β levels (855 ± 87.5 pg/mL) decreased significantly ($P < 0.0001$), as shown in Figure 5.3b. The raised concentration of IL-1β is associated with invasiveness and aggressiveness of breast cancer and higher tumor grade. The diseased control group shows IL-6 (2200.6 ± 69 pg/mL) concentration significant ($P < 0.0001$) rise in the serum. However, the Meth-Cs-NPs treatment group indicated IL-6 levels (1515 ± 53 pg/mL) are significant ($P < 0.01$) decreases in serum. Whereas in the free MTX treatment group, IL-6 level (1881 ± 19.1 pg/mL) is significantly reduced ($P < 0.0001$) as shown in Figure 5.3c. IL-6 is a pleiotropic cytokine [275] that affects cell development

and differentiation. TNF-α and IL-6 promote non-cancerous cells' transformation into tumor cells, which help in the growth of tumors [276]. The results demonstrate that MNU-induced rats had significantly ($p < 0.001$) higher concentrations of the cytokines, TNF-α, and Interleukins (IL) (1β & 6). At the same time, treatment groups showed a considerable reduction in these levels.

Table 5.1. *Effect of MTX on pro-inflammatory cytokines levels in treatment groups.*

Cytokines	Normal control	Diseased control (MNU only)	Meth-Cs-NPs	Cs-NPs	MTX
TNF-α (pg/mL)	12.6±1.08	36.9±5	17.31±1.15	33.09±1.25	21±1.87
IL-1β (pg/mL)	223.3±60.2	1540±131.1	433.3±66.5	1362±66.36	855±87.5
IL-6 (pg/mL)	1101±31	2200.6±69	1515±53	2033.3±81.1	1881±19.1

Tumor Necrosis Factor-α (TNF-α) and Interleukins (IL-1β & IL-6) Data expressed as mean ± S.d, n =3.

5.3.3 Role of MTX-loaded nanoparticles in tumor suppression

The primary activity of methotrexate (MTX), a folate antagonist, has been thought to be in oncology. Since folates are the essential building blocks for maintaining cell growth, it has an antifolate effect [277]. Because the oncologic mechanism prevents the production of pyrimidines and purines, the cell cycle's S phase is disrupted, leading to cell death [278]. The primary enzymes that MTX inhibits are 5-aminoimidazole-4-carboxamide ribonucleotide (AICAR) [279] transformylase (ATIC) and block the enzyme dihydrofolate reductase (DHFR), which catalyzes the change of dihydrofolate to tetrahydrofolate [280].

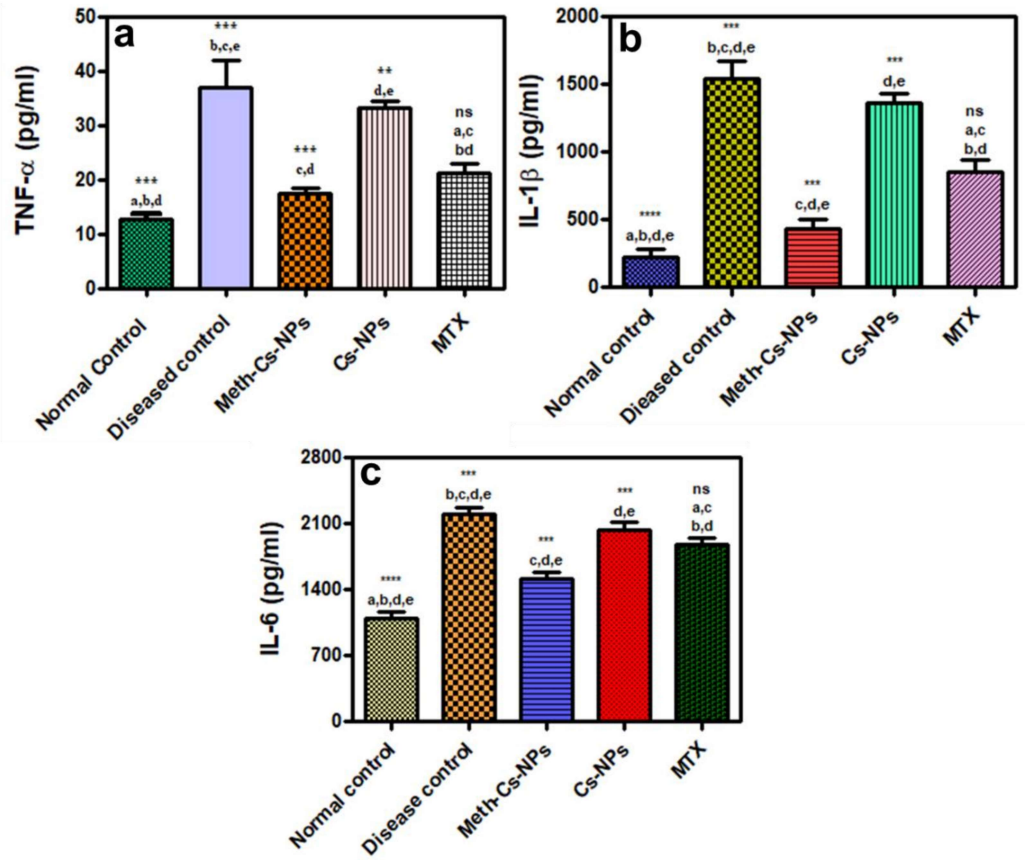

Figure 5.3: *Effect of Meth-Cs-NPs on pro-inflammatory cytokine. One-way ANOVA followed by Dunnett's post-test analyzed results; All groups were compared with the normal control group. Where a; Normal control, b; Disease control, c; free MTX, d; Cs-NPs, and e; Meth-Cs-NPs. (***p < 0.0001), (**p < 0.001) and (*p < 0.05). Data expressed as mean ± S.d, n =3.*

The reaction's final product inhibits thymidylate synthetase (TYMS), essential for synthesizing thymidine residues. Raising the level of UTP and lowering the level of ATP and GTP has depleted the purine and pyrimidine pool in T-cells simultaneously [281]. T-cells, monocytes, and neutrophils are all influenced by MTX in their ability to produce reactive oxygen species (ROS). It promotes apoptosis while preventing T-cell proliferation [282]. The production of pyrimidines and purines (de novo), as well as Nuclear factor kappa B (NF-κB) activation [283], were thought to be inhibited by MTX,

which would result in the inhibition of cytokines. The capability of MTX to inhibit the early development of T & B cells and to suppress the inflammatory mediators, TNF-α, IL-1β, and IL-6, that regulate the immune response. Nuclear factor kappa B activation is necessary for these mediators' transcription [284]. Inflammation, immunological response, cell proliferation, and apoptosis [285] are all regulated by the cytoplasmic transcription factor (NF-κB). The anti-inflammatory effects of MTX may be achieved by inhibiting NF-κB signaling. As a result, the cytokines, including TNF-α, IL-1β, and IL-6, were significantly ($p < 0.001$) reduced when treated with nanoparticles. So, from this work, we can comprehend the role that methotrexate-loaded chitosan nanoparticles affect cytokine modulation. The Proposed mechanism of Methotrexate **(**MTX) is shown in Figure 5.4. Although results are encouraging, further investigations are required to determine how Meth-Cs-NPs affect the biomarkers that the liver and kidneys secrete. These biomarkers may indicate the organs' proper functioning, but their up-and-down-regulation could be correlated with tumor growth and suppression. In summary, our results showed that nanoparticles significantly attenuated the expression of cytokines in the MNU-induced mammary tumor. As a result of the findings, Meth-Cs-NPs appeared to be a viable candidate for new inflammatory inhibitors.

5.3.4 Role of Meth-Cs-NPs on hepatic & renal biomarker regulation

The change in biochemical enzymes in the different treatment groups after the completion of the experiment (Figure 5.5 and Table 5.2). The kidney function test shows that in the diseased control group, the ALP (403 ± 14), Urea (113±6), and Creatinine (2±0.05), whereas in the Meth-Cs-NPs treated group shows that ALP (244±15), Urea (56.62±5) and Creatinine (0.81±0.058) levels were reduced. However, the Meth-Cs-NPs treatment group indicates the concentration of ALP, Urea, and Creatinine is nearly similar to the normal control groups (Table: 5.2).

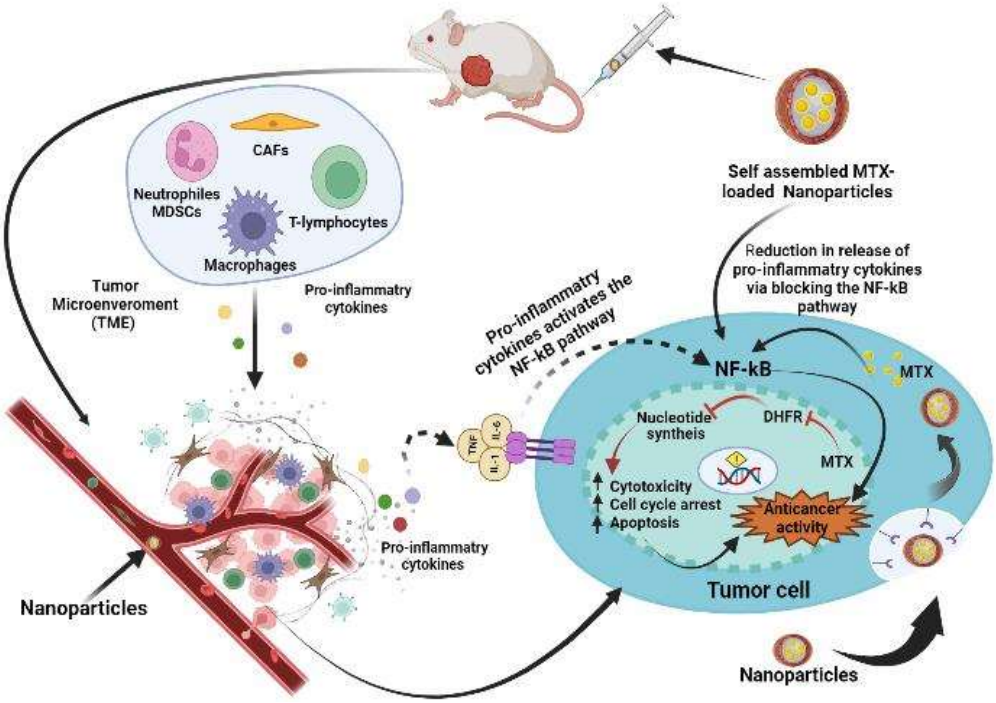

Figure 5.4: *Proposed mechanism of Methotrexate (MTX) blocks the primary enzyme dihydrofolate reductase (DHFR), which changes the dihydrofolate to tetrahydrofolate. The de novo synthesis of purines and pyrimidines, as well as nuclear factor kappa B (NF-κB) activation, were thought to be inhibited by MTX, which would result in the inhibition of cell proliferation (T & B) and cytokines expression. Inflammation, immunological response, cell proliferation, and apoptosis are regulated by the cytoplasmic transcription factor nuclear factor kappa B (NF-κB). The anti-inflammatory effects of MTX may be achieved by inhibiting NF-κB signaling. As a result, the cytokines, including TNF-α, IL-1β, and IL-6, were reduced when treated with nanoparticles.*

The results suggested that Meth-Cs-NPs was non-toxic after i.v injection and can protect tissues from the toxic effects of free MTX. The free MTX treatment group significantly raised Urea and Creatinine levels compared to normal control groups. The ALP, Urea, and Creatinine concentration in Meth-Cs-NPs treatment groups was low compared to free MTX and diseased control groups. According to the findings, kidney tissues were significantly protected by MTX-loaded nanoparticles. The histological changes found in the kidney after MTX treatment supported the biochemical alterations seen in the rats.

The liver function test (SGOT and SGPT) indicated that biochemical parameters decreased significantly in the Meth-Cs-NPs treated group (Table 5.2). All biochemical parameters were elevated in the diseased control group compared to the treated groups; free MTX, Cs-NPs, and Meth-Cs-NPs. However, among the treated groups, Meth-Cs-NPs performed best and showed a significantly decreased in levels of biochemical markers. The Meth-Cs-NPs were safe due to their biocompatible nature of polymer and encapsulation of methotrexate inside the nanocarrier, compared to the free methotrexate (MTX). Liver and kidney function tests and histology studies have justified the toxicity and safety profile of the nanoparticles. The Meth-Cs-NPs have reportedly achieved a similar therapeutic response to that of treatment as reported studies on gold nanoparticles (GNPs) [286–288].

Table 5.2. *Effect of MTX on biochemical marker levels in experimental groups.*

Parameters	Normal control (NC)	Diseased control (DC)	Free MTX	Cs-NPs	Meth-Cs-NPs
Urea (mg/dl)	53.73±4	113±6	93±4.5	84±6	56.62±5
Creatinine (mg/dl)	0.66±0.060	2±0.05	1.8±0.059	1.40±0.068	0.81±0.058
ALP (U/L)	239±15	403±14	335±15	298±12	244±15
SGPT (U/L)	38±2	84±1.9	48±2.1	65±2.5	42±1.8
SGOT (U/L)	12±1.9	55±4	26±2.2	38±3	15±2

ALP = Alkaline phosphatase, SGPT = Serum glutamic pyruvic transaminase, SGOT = serum glutamic-oxaloacetic transaminase. (Data expressed as mean ± S.d, n =3).

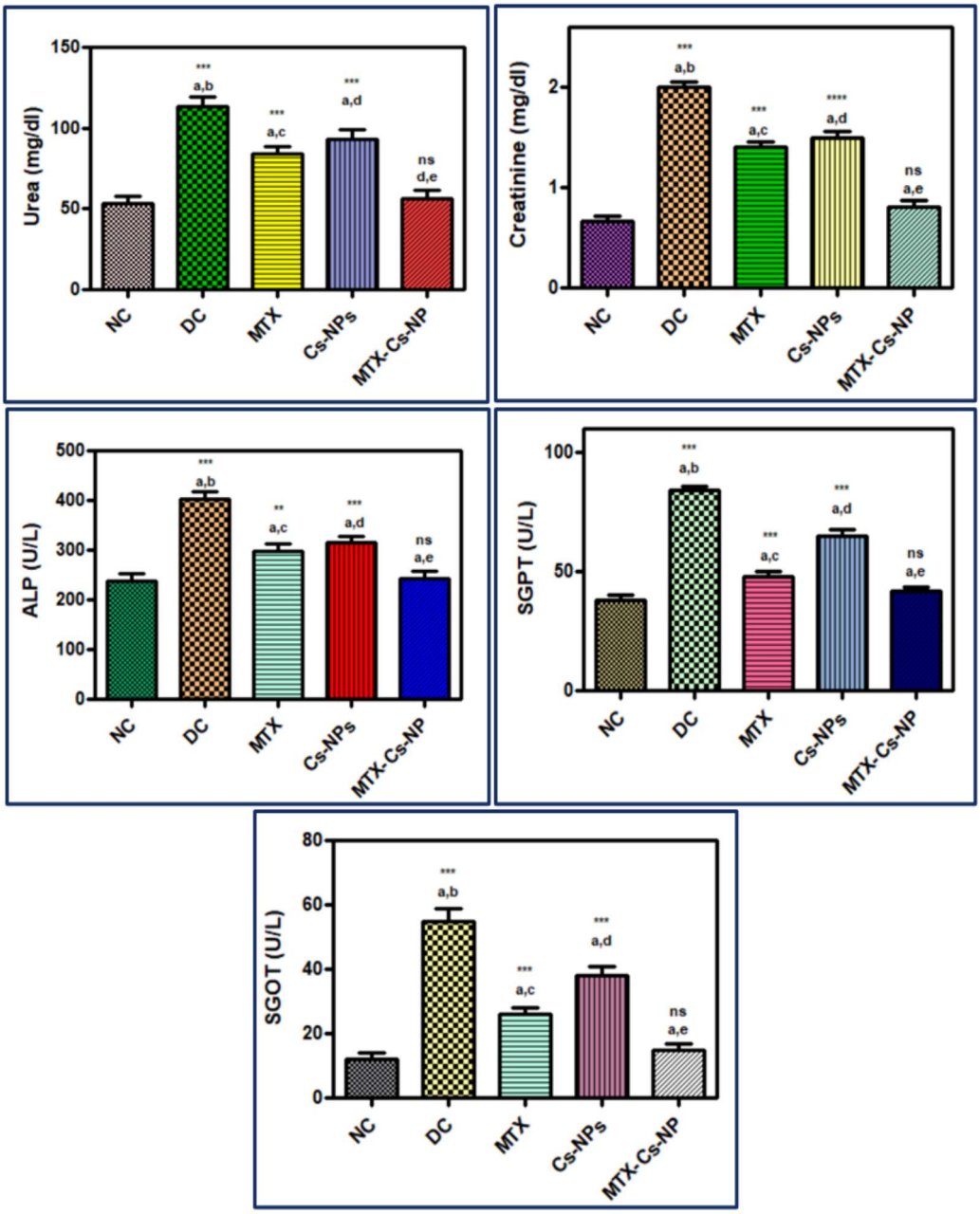

Figure 5.5: *The level of Biochemical markers in the serum of different groups. One-way ANOVA followed by Dunnett's post-test analyzed results; All groups were compared with the normal control group (NC). a; Normal control, b; Disease control (DC), c; free MTX, d; Cs-NPs and e; Meth-Cs-NPs. (***p < 0.0001), (**p < 0.001) and (*p < 0.05), (Data expressed as mean ± S.d, n =3).*

5.3.5 Tumor Histologypathology (after treatments)

Post-treatment histological alterations in tumor morphology are critical in assessing the therapeutic response. The antitumor efficacy of nanotherapeutics in tumor-bearing rats was evaluated. Results show that the aggregation of macrophages was present in the stroma and parenchyma of the mammary tumors in both treated and non-treated groups. However, these needed to be more evident in the treated ones. The histopathology of the diseased control group exhibited more malignancy as the tumor grew and behaved more aggressively with time (Figure 5.2). Unlike free MTX treatment groups (Figure 5.6a), the Meth-Cs-NPs-treated group tumor became less aggressive (Figure 5.6b). The carcinoma exhibited epithelial clusters encircled by intense desmoplasia. Lower histological grade of cancer with cytoplasmic vacuolization in cancer cells and less necrosis implicates the positive efficacy of Meth-Cs-NPs.

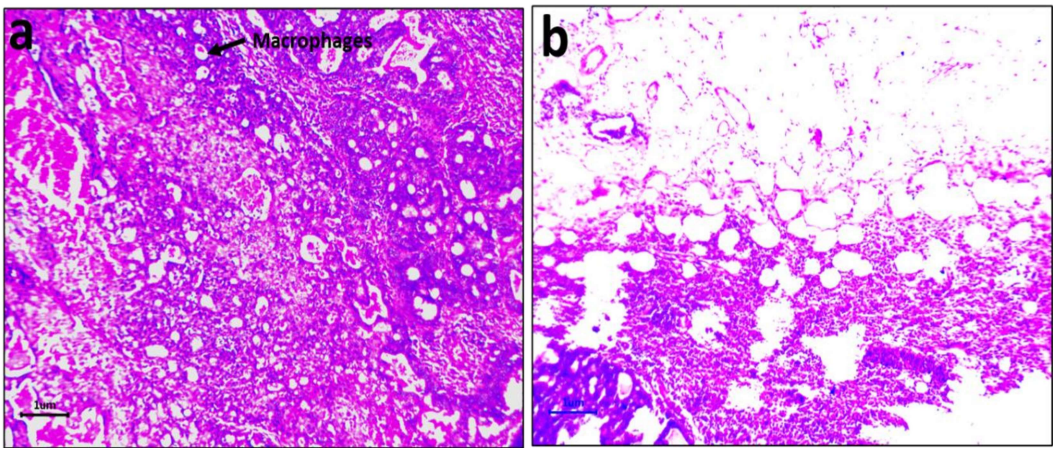

Figure 5.6: *Histopathology shows the mammary tumor of rat (MNU-induced) after treatment; (a) free MTX treated mammary tumors and (b) Meth-Cs-NPs treated mammary tumors. H&E staining, bar size 1µm with 10X magnification.*

5.3.6 Effect of Meth-Cs-NPs on Kidney (Histopathology)

The histological evaluation of the kidneys of rats in all treatment groups using Haematoxylin and Eosin (H&E staining). Figure 5.7 shows the histological alterations in the rat kidneys of the various treatment groups. In the Normal control group, the kidney exhibits normal morphology with an intact glomerulus (GLM), proximal and distal tubules (PT), and tubular cells that are intact and normal in their nuclei. Diseased control group: The cortical region showed tubular necrosis, congestion, enlarged Bowman's space, and lymphocytic infiltration. Tubular degeneration (TD) and cytoplasmic vacuolation are visible in the medullary area. Leukocyte infiltration, edema exudate, and necrotic foci were present in the group treated with free MTX. The tubular cells have a slight to moderate deterioration. Proximal and distal tubules show normal histology in the Cs-NPs treated group. There is a slight tubular degeneration at the focal sites. Glomerulus and Bowman's capsules in the group that received Meth-Cs-NPs appear healthy.

5.3.7 Effect of Meth-Cs-NPs on Liver (Histopathology)

The histological changes observed in the liver of rats in the different treatment groups; a) Normal morphology of liver tissue in the normal control group, b) The sinusoids around the significant veins were noticeably expanded in the diseased control group after MNU treatment, which was distorted by multifocal mononuclear cell infiltrations (black arrow), c) Comparable to the normal control group, the free MTX treatment group displayed similar patterns, but with less mononuclear cell infiltration (black arrow), d) Normal liver tissue morphology was seen in the Cs-NPs treated group, much like in the control group, and e) Normal morphology of liver tissue in the Meth-Cs-NPs treated group, same like in the control group.

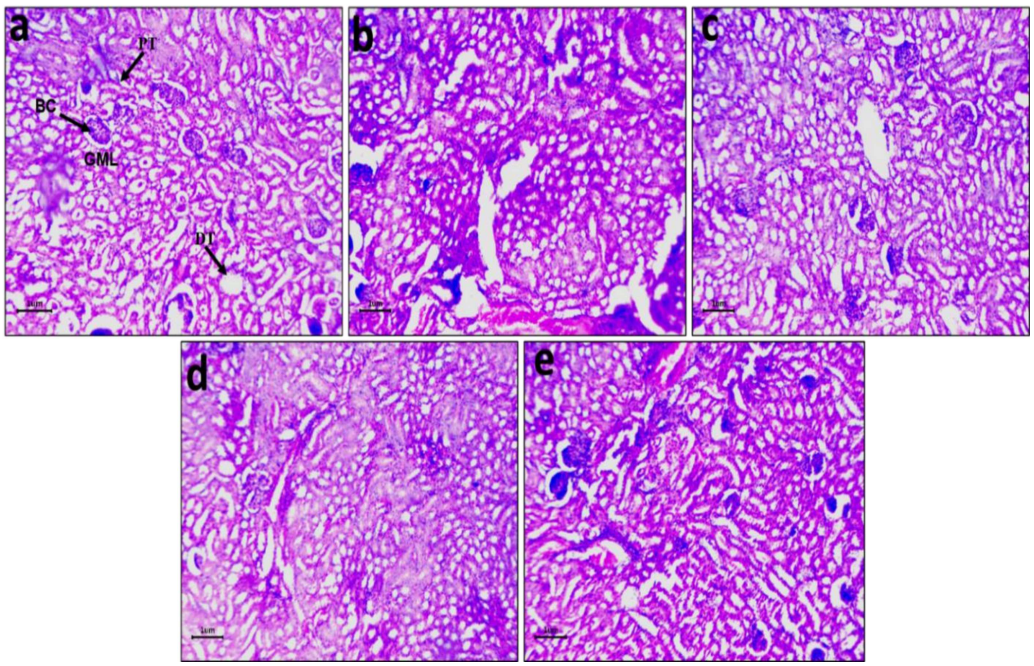

Figure 5.7: *Histopathological of kidney section from control and different treatment groups;* ***(a)*** *Normal control,* ***(b)*** *Diseased control,* ***(c)*** *Free MTX,* ***(d)*** *Cs-NPs,* ***(e)*** *Meth-Cs-NPs treated groups. H&E staining, bar size 1µm with 10X magnification. GML; Glomerulus, BC; Bowman's capsule, PT; Proximal tubules, DT; Distal tubules.*

Histological findings show that rats exposed to MNU showed more significant deterioration, and necrosis of the liver tissues increased with time (Diseased control). Comparing the livers of the rats in the Meth-Cs-NPs treatment group to those in the MNU group, regenerative alterations were found. According to histopathological findings, Meth-Cs-NPs may lessen the liver damage caused by MNU by preventing changes in the portal area and stifling necrosis-causing activities. These findings support the hypothesis that chitosan nanoparticles loaded with MTX exhibit low systemic toxicity and are biocompatible in systemic circulation. The results indicate that Meth-Cs-NPs nanoparticles can be employed as a breast cancer preventive medicine by minimizing the side effects of MTX when loaded in a polymeric nanocarrier (Figure 5.8).

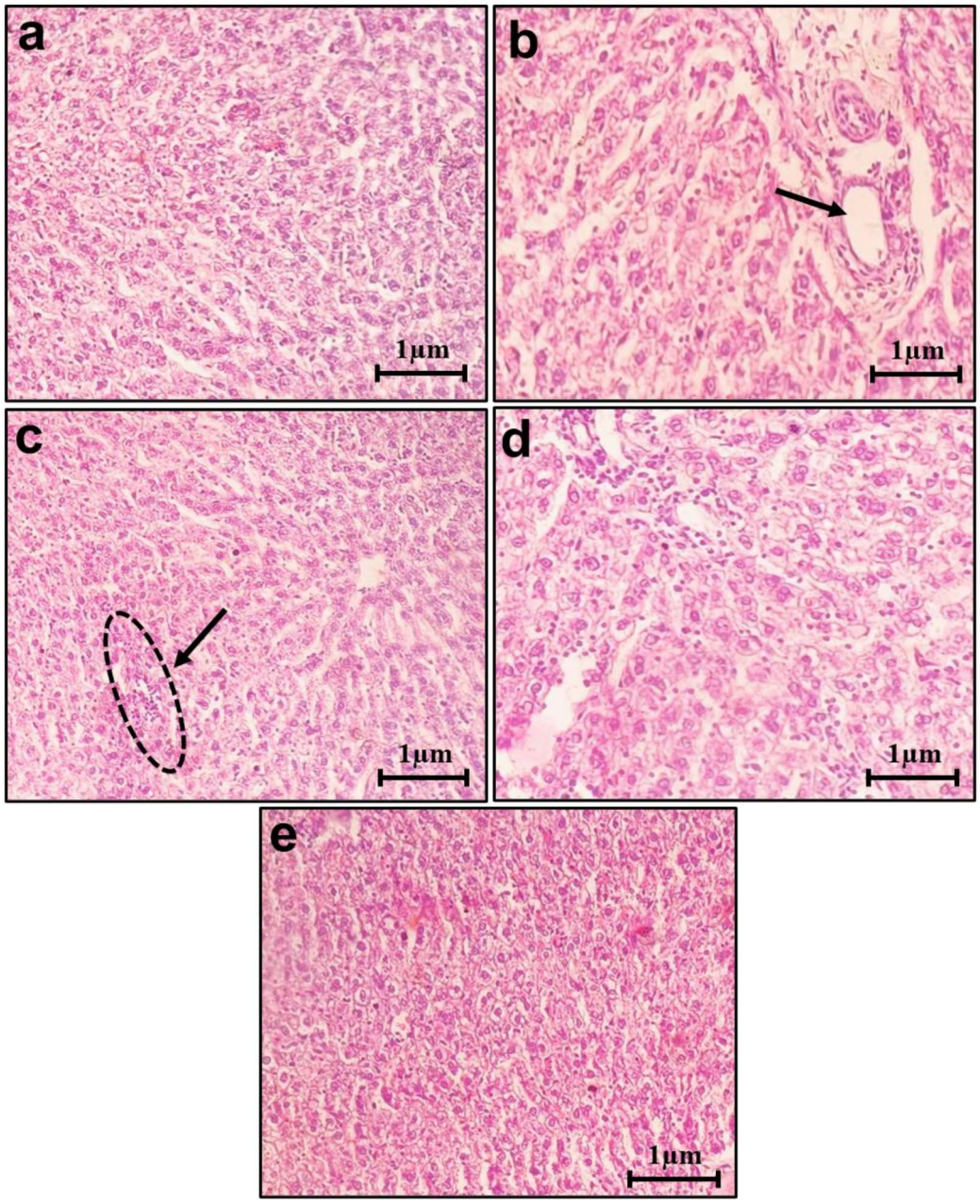

Figure 5.8: *Histopathological of liver section from control and different treatment groups;* ***(a)*** *Normal control group,* ***(b)*** *Diseased control group (multifocal mononuclear cell infiltrations indicated by black arrow),* ***(c)*** *Free MTX treatment group (mononuclear cell infiltration indicated by black arrow)* ***(d)*** *Cs-NPs treatment group and* ***(e)*** *Meth-Cs-NPs treatment group. H&E staining (Haematoxylin and Eosin) bar size 1µm with 20X magnification.*

5.4 Conclusion

A versatile multifaceted methotrexate molecule having targeting and anticancer treatment potential was encapsulated in chitosan and examined for breast cancer treatment. We show that in-vivo application of formulated nanoparticles, which down-regulates pro-inflammatory cytokines and lowers ALP, Urea, creatinine, SGPT, and SGOT, were comparable to diseased control rats. Our experiment shows that the new formulation Meth-Cs-NPs has significant anticancer efficacy with low cytotoxicity compared to free Methotrexate. We conclude that this Meth-Cs-NPs anticancer.